Quinones and nitroaromatic compounds as subversive substrates of Staphylococcus aureus flavohemoglobin

Myriam Moussaoui, Lina Misevičienė, Žilvinas Anusevičius, Audronė Marozienė, Florence Lederer, Laura Baciou, Narimantas Čėnas

Quinones and nitroaromatic compounds as subversive substrates of *Staphylococcus aureus* flavohemoglobin

Myriam Moussaoui[a], Lina Misevičienė[b], Žilvinas Anusevičius[b], Audronė Marozienė[b], Florence Lederer[a], Laura Baciou[a], Narimantas Čėnas[b,*]

[a] *Laboratoire de Chimie Physique, Université Paris Sud, CNRS UMR 8000, 91405 Orsay Cedex France*
[b] *Institute of Biochemistry of Vilnius University, Saulėtekio 7, LT-10257 Vilnius, Lithuania*

Free Radical Biology and Medicine 123 (2018) 107–115 https://doi.org/10.1016/j.freeradbiomed.2018.05.071

E-mail address: narimantas.cenas@bchi.vu.lt (N. Čėnas).

* Corresponding author.

Keywords:
Flavohemoglobins
Staphylococcus aureus
Quinones
Nitroaromatic compounds
Nitrosative stress

A B S T R A C T

In microorganisms, flavohemoglobins (FHbs) containing FAD and heme (Fe^{3+}, metHb) convert NO. into nitrate at the expense of NADH and O_2. FHbs contribute to bacterial resistance to nitrosative stress. Therefore, inhibition of FHbs functions may decrease the pathogen virulence. We report here a kinetic study of the reduction of quinones and nitroaromatic compounds by *S. aureus* FHb. We show that this enzyme rapidly reduces quinones and nitroaromatic compounds in a mixed single- and two-electron pathway. The reactivity of nitroaromatics increased upon an increase in their single-electron reduction potential (E_7^1), whereas the reactivity of quinones poorly depended on their E_7^1 with a strong preference for a 2-hydroxy-1,4-naphthoquinone structure. The re-action followed a 'ping-pong' mechanism. In general, the maximal reaction rates were found lower than the maximal presteady-state rate of FAD reduction by NADH and/or of oxyhemoglobin ($HbFe^{2+}O_2$) formation (~130 s^{-1}, pH 7.0, 25 °C), indicating that the enzyme turnover is limited by the oxidative half-reaction. The turnover studies showed that quinones prefreqently accept electrons from reduced FAD, and not from $HbFe^{2+}O_2$. These results suggest that quinones and nitroaromatics act as 'subversive substrates' for FHb, and may enhance the cytotoxicity of NO. by formation of superoxide and by diverting the electron flux coming from reduced FAD. Because quinone reduction rate was increased by FHb inhibitors such as econazole, ketoconazole, and miconazole, their combined use may represent a novel chemotherapeutical approach.

1. Introduction

Flavohemoglobins (FHbs) have been found in a wide variety of bacteria and fungi [1,2]. They play a key role in the bacterial resistance to nitrosative stress and in the modulation of NO. signaling (reviewed in [3,4]). FHbs consist of an *N*-terminal heme-binding domain and of *C*-terminal FAD- and NAD-binding modules [5,6]. These modules present homology with ferredoxin:$NADP^+$ reductase (FNR). During turnover, in the reductase domain, NADH reduces FAD, which further reduces the Fe^{3+}-form of the hemoglobin (methemoglobin, $HbFe^{3+}$) of the globin domain; oxyhemoglobin ($HbFe^{2+}O_2$) is finally formed under aerobic conditions. The reaction of the $HbFe^{2+}O_2$ moiety of FHb with $NO^{\cdot}$ leads to $NO^{\cdot}$ detoxification, *i.e.,* the formation of nitrate (NO_3^-) [7] instead of the toxic peroxynitrite ($ONOO^-$), which is formed in the reaction of $NO^{\cdot}$ and superoxide ($O_2^{-\cdot}$). The key role of FHbs in the neutralization of $NO^{\cdot}$ action is mainly due to their high catalytic activity (a turnover rate of *ca.* 100 s^{-1}), and their ability to bind $NO^{\cdot}$ at sub-micromolar concentrations [8]. Because of the sensitivity to oxidative- and nitrosative stress of human respiratory tract invasion by the *Pseudomonas aeruginosa* and *Escherichia coli* pathogenic strains [9,10], FHbs can also be considered as virulence factors for bacterial pathogens. *Staphylococcus aureus* infections represent a serious worldwide challenge [11]; this pathogen escapes innate immunity due to its capacity to neutralize $NO^{\cdot}$ and nitrosative stress [12,13]. In particular, transcription of the FHb mRNA in *S. aureus* is upregulated by the nitrosative stress in an oxygen dependent manner [14].

Because FHbs are not present in mammals, inhibiting them or subverting their functions may be an efficient approach to decrease the virulence of pathogens. Azole antibiotics such as miconazole, econazole, or ketoconazole are used in the treatment of fungal and bacterial infections; they are known as inhibitors of P-450 cytochromes ([15,16], and references therein). In addition, they are efficient FHb inhibitors

Abbreviations: $ArNO_2$, aromatic nitrocompound; E_7^1, single-electron reduction potential at pH 7.0; FNR, ferredoxin:$NADP^+$ reductase; FHb, flavohemoglobin; Hb, hemoglobin; $HbFe^{2+}O_2$, oxyhemoglobin; metHb, methemoglobin; Q, quinone; P-450R, NADPH:cytochrome P-450 reductase; *S. aureus*, *Staphylococcus aureus*; *Sa*FHb, *S. aureus* flavohemoglobin; TNT, 2,4,6-Trinitrotoluene

[14,17–19] by binding to the enzyme heme moiety. This decreases the rate of NO. neutralization, modulates the FHb-catalyzed formation of $O_2^{-\cdot}$ [20], and increases the intracellular oxidative stress in *S. aureus* [14].

Quinones (Q) and nitroaromatic compounds ($ArNO_2$) are widely used as oxidizing substrates in the studies of flavoproteins redox reactions. Among their advantages, one could mention the well characterized thermodynamics of single- and two-electron reduction of quinones (reviewed in [21]), as well as the applicability of the Marcus model to the single-electron reduction of quinones and nitroaromatics ([22,23], and references therein). Moreover, quinones and nitroaromatic compounds frequently possess cytotoxic, antitumor, antiparasitic, and antibacterial properties. This is partly due to the redox cycling of their free radicals, $Q^{-\cdot}$ and $ArNO_2^{-\cdot}$, which leads to 'oxidative stress', *i.e.,* enhanced production of $O_2^{-\cdot}$, H_2O_2 and hydroxyl radical ($OH^{\cdot}$) ([21,23–25], and references therein). Their free radicals are formed during their single-electron reduction by flavoenzymes such as NADPH:cytochrome P-450 reductase (P-450R) or FNR, or by FeS-containing redox carriers [26–29].

The reactions of FHbs with quinones and nitroaromatic compounds have not been characterized so far, although they may be important due to the possibility of a single-electron reduction of these compounds which may lead to their redox cycling. In addition, the subsequent reaction of the overproduced $O_2^{-\cdot}$ with $NO^{\cdot}$ may enhance the formation of cytotoxic $ONOO^-$. Thus, these compounds could act as "subversive substrates" for FHbs, transforming their protective functions into cytotoxic ones. In this work, we have characterized the mechanisms of reduction of quinones and nitroaromatic compounds by *Staphylococcus aureus* flavohemoglobin using steady- and presteady-state kinetic methods.

2. Material and methods

2.1. Reagents

NADH, NAD^+, cytochrome *c*, superoxide dismutase, azole compounds, quinones and nitroaromatic compounds were obtained from Sigma-Aldrich. 2,4,6-Trinitrotoluene was a generous gift of Dr. Jonas Šarlauskas (Institute of Biochemistry, Vilnius).

2.2. Production and purification of S. aureus recombinant FHb

Competent BL21(DE3) cells were purchased from Life Technologies, France. Chromatographic separations were carried out using DEAE Fast Flow Sepharose CL-6B and Superdex ™ 75 resins from GE Healthcare (France). All reagents were purchased from Sigma Aldrich (France) unless specifically mentioned.

The plasmid construction coding for *Sa*FHb was described previously [20]. The protocols for protein expression and purification of recombinant *Sa*FHb were adapted from those used for yeast FHb [19] as previously described [20]. The protein purity was analyzed by 10% SDS-PAGE. Protein concentration was assayed by two methods: the bicinchoninic acid method with BSA as standard [30], and spectrophotometrically, by the oxidized heme concentration on a double beam Uvikon 943 spectrophotometer (Kontron Instruments, Milan, Italy), using $\varepsilon_{400} = 90\,mM^{-1}\,cm^{-1}$ [20].

2.3. Steady-state kinetic studies

The steady-state reactions of *Sa*FHb with quinones or nitroaromatic compounds were carried out in 0.1 M K-phosphate buffer (pH 7.0) containing 1 mM EDTA at 25 °C using a Uvikon 943 spectrophotometer, by following the rate of NADH oxidation ($\Delta\varepsilon_{340} = 6.2\,mM^{-1}\,cm^{-1}$). In these cases, the rate of an intrinsic NADH-oxidase activity of *Sa*FHb, $0.06\,s^{-1}$, was substracted. The values of turnover rate, k_{cat}, reflecting the maximal number of moles NADH oxidized per mole of the enzyme active center per second, and k_{cat}/K_m, the apparent bimolecular rate constant, correspond to the inverse intercepts and slopes in Lineweaver-Burk coordinates, [E]/*v vs.* 1/[Q] or 1/[$ArNO_2$]. These rate constants were obtained by fitting the experimental data to the Michaelis-Menten equation using the Kaleidagraph software. In the case of two-substrate reactions, the data were fitted to Eq. (1) corresponding to the ‚ping-pong' kinetic mechanism, where [NADH] stands for [S]:

$$\frac{V}{[E]} = \frac{k_{cat}[S][Q]}{K_{m(S)}[Q] + K_{m(Q)}[S] + [S][Q]} \quad (1)$$

For the inhibition study at fixed concentration of NADH and varied concentration of quinone or *vice versa*, the data were fitted to Eqs. (2,3), which describe competitive and uncompetitive inhibition by the reaction product NAD^+ [I], respectively. The inhibition constants K_{is} and K_{ii} describe the effects of inhibitors on the slopes and the *y*-axis intercepts in the Lineweaver-Burk plots, respectively:

$$\frac{V}{[E]} = \frac{k_{cat}\ [S]}{K_{m(S)}\left(1+\frac{[I]}{K_{is}}\right)+[S]}, \quad (2)$$

$$\frac{V}{[E]} = \frac{k_{cat}\ [S]}{K_{m(S)}+[S]\left(1+\frac{[I]}{K_{ii}}\right)}, \quad (3)$$

In the studies of *Sa*FHb activity in the presence of azole compounds, the data were fitted to Eq. (4):

$$\frac{V}{[E]} = \frac{k_{cat}\ [S]}{\alpha K_m\left(\frac{K_a+[A]}{\alpha K_a+[A]}\right)+[S]}, \quad (4)$$

where α is the maximal degree of K_m decrease in the presence of compound (A), and K_a is the activator binding constant [31]. In separate experiments, the reaction rate was monitored as the reduction of added 50 μM cytochrome *c* ($\Delta\varepsilon_{550} = 20\,mM^{-1}\,cm^{-1}$). The rates of quinone- or nitroaromatic-mediated reduction of cytochrome *c* were obtained after the substraction of the intrinsic cytochrome *c* reduction rate by /*Sa*FHb, obtained in the absence of Q or $ArNO_2$.

2.4. Aerobic presteady-state kinetic studies

The experiments were performed at 25 °C in 0.1 M K-phosphate buffer, 1 mM EDTA, pH 7.0, using a SX20 stopped-flow spectrophotometer (Applied Photophysics, UK) equipped with a diode array. The syringes contained *Sa*FHb (5–6 μM after mixing) and NADH (50–500 μM after mixing). The *Sa*FHb reduction by NADH was analyzed using a two-exponential fit with a rapid phase corresponding to *ca.* 80% of the absorbance change at selected wavelengths. In the turnover studies, the enzyme in the first syringe (5 μM after dilution) was mixed with the contents of the second syringe (100 μM NADH and 50–150 μM 1,4-naphthoquinone after dilution). The results were analyzed at several wavelengths as specified in the Results section.

2.5. Anaerobic presteady-state kinetic studies

The anaerobic kinetic studies of *Sa*FHb reduction by NADH were performed with similar concentrations of protein and NADH as for the aerobic experiments. Buffers and substrate solutions were purged for 20 min with Ar from which oxygen has been scrubbed by an Althech Big Oxygen Trap. The concentrated enzyme was separately ventilated without bubbling, and was finally diluted with the relevant deaerated buffer. At the last minute, before mixing enzyme and NADH, small volumes (~1%) of protocatechuate and protocatechuate dioxygenase were added to a final concentration of 0.4 mM and 6.0 μg/ml in order to remove the last traces of oxygen [32].

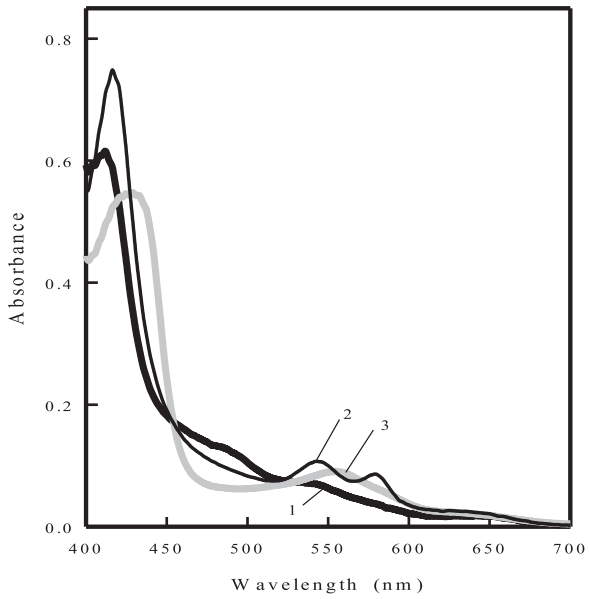

Fig. 1. Absorption spectra of *S.aureus* FHb under various redox states. The spectra of 6.0 μM *Sa*FHb: (1) oxidized, (2) reduced under aerobic conditions, and (3) reduced under anaerobic conditions. Spectra (2 and 3) were recorded after an enzyme incubation of 20 min in the presence of 200 μM NADH.

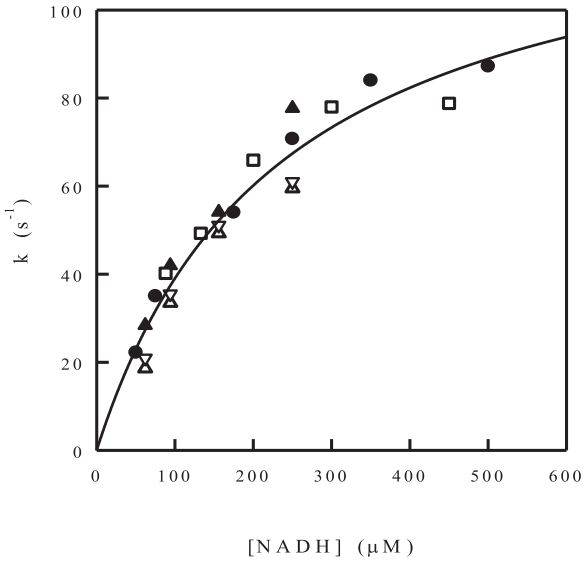

Fig. 2. Dependence on NADH concentration of *Sa*FHb presteady-state reduction rate constants for prosthetic groups under aerobic and anaerobic conditions. The kinetics were monitored at 480 nm in anaerobic (upward filled triangles) and aerobic conditions (filled circles), at 580 nm in anaerobic (upward blank triangles) and aerobic conditions (blank squares), and at 430 nm in anaerobic conditions (downward blank triangles).

3. Results

3.1. Presteady-state kinetics of SaFHb reduction by NADH

The first aim of our study was to establish which active center of *Sa*FHb, reduced FAD or oxyhemoglobin ($HbFe^{2+}O_2$), or both, is responsible for the reduction of quinones. For this purpose, we initially examined the spectral properties of reduced forms of *Sa*FHb. The *Sa*FHb reduction by excess NADH under aerobic or anaerobic conditions leads to the appearance of absorbance maxima at 414 nm, 542 nm, and 580 nm (formation of oxyhemoglobin), or at 430 nm and 560 nm (formation of deoxyhemoglobin, $HbFe^{2+}$), respectively (Fig. 1). These spectral changes are analogous to those of *E. coli* [8] and *S. aureus* [20,33] FHbs after the reduction under various conditions. Although the spectra are characterized by an isosbestic point at 460 nm, which corresponds to λ_{max} of oxidized FAD, the reduction of FAD is evidenced by a significant absorbance decrease at 470–500 nm (Fig. 1). The two electrons given by NADH will be initially distributed between the flavin and the heme leading to $FADH^{\cdot}$ and Fe^{2+}; thus $FADH^{\cdot}$ may contribute to an increase in absorbance at 550–600 nm. The $FADH^{\cdot}$ species with λ_{max} ~ 600 nm are transiently formed during the pulse-radiolysis of *Ralstonia eutropha* FHb [34]. However, the semiquinone state of FHb is unstable since the FAD of *Sa*FHb behaved as an obligatory two-electron acceptor during potentiometric titrations [33]. Thus, we believe that spectra 2 and 3 in Fig. 1 correspond to the fully ($3e^-$)-reduced *Sa*FHb forms. In this context, we analyzed the presteady-state reduction of the enzyme by NADH at selected wavelengths by following: *a*) the absorbance increase at 580 nm under the aerobic conditions (the formation of $HbFe^{2+}O_2$), and under anaerobic conditions; *b*) the absorbance decrease at 480 nm under aerobic or anaerobic conditions (reduction of FAD), and *c*) the formation of $HbFe^{2+}$ monitored at 430 nm under anaerobic conditions. The reactions proceeded biphasically with a rapid phase corresponding to ~80% of the total absorbance change, and a subsequent slow phase (data not shown). The similar biphasic kinetics were observed during the reduction of *E. coli* FHb, and were tentatively ascribed to slow interprotein electron exchange [8]. The further elucidation of the above phenomena is an object of our future studies. Our data show that all the rate constants corresponding to the fast phase roughly follow the same dependence on NADH concentration, and there is no significant difference between the rate constants for the reduction of FAD or heme, or the formation of $HbFe^{2+}O_2$ (Fig. 2). When monitoring the fast reduction of *Sa*FHb, no transient absorbance increase and decrease at ≥ 600 nm was observed, suggesting the absence of transient FADH. formation. This is in line with the kinetic data of *E. coli* FHb reduction [8]. Thus, our data show that the reduction of FAD is the rate-limiting step in

catalysis, and that the subsequent steps, *i.e.,* the heme reduction by the reduced FAD, and the formation of $HbFe^{2+}O_2$, proceed much faster. At infinite NADH concentration, the maximal reduction rate of FHb is 130.5 ± 10 s^{-1}, and the apparent k_{cat}/K_m value for NADH is 5.6 ± 0.4 × 10^5 M^{-1} s^{-1}.

3.2. Kinetics of SaFHb under multiple turnover conditions

We found that 1,4-naphthoquinone behaved as one of the best electron acceptors for *Sa*FHb. It did not absorb at 480–580 nm, and its semiquinone and two-electron reduced forms are rapidly reoxidized by oxygen [21]. We performed multiple turnover studies of *Sa*FHb in the presence of NADH and 1,4-naphtoquinone under aerobic conditions (Figs. 3 and 4). We assume that the absorbance changes at 480 nm are mainly due to FAD reduction, and that the absorbance changes at 580 nm are mainly due to $HbFe^{2+}O_2$ formation. Our data show that the initial fast phase of absorbance decrease at 480 nm mainly attributed to FAD reduction by NADH is followed by a rapid reoxidation starting at *ca.* 0.2 s (Fig. 3A), and reaching 60–75% reoxidation at 1.0 s, and 80–93% at 20 s, depending on the oxidant concentration (Fig. 3B).

In contrast, the enzyme absorbance changes at 580 nm under the same conditions follow a different time course: the fast phase absorbance rise attributed mainly to heme reduction ($HbFe^{2+}O_2$ formation) and possibly to FADH. formation is followed by a quasi-steady-state phase with a decreased steady-state concentration of intermediates (5–7 s), and a subsequent slower reoxidation of $HbFe^{2+}O_2$ (30–40% reoxidation at 20 s (Fig. 4A and B)). It can be seen that 1,4-naphthoquinone slows down the initial formation of $HbFe^{2+}O_2$ (Fig. 4A), evidently intercepting electrons from the reduced FAD. Taken together, these data imply that under the aerobic turnover conditions in the presence of quinone, the reduced FAD reaches much more rapidly the

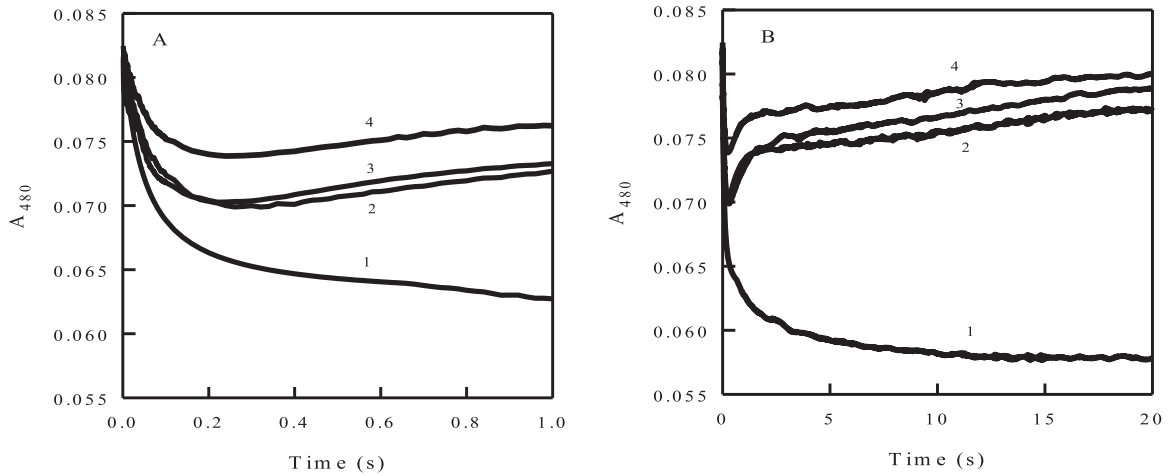

Fig. 3. Turnover of SaFHb in the presence of NADH and 1,4-naphthoquinone under aerobic conditions monitored at 480 nm. The reduction of *Sa*Fhb FAD (5.0 μM) by 100 μM NADH (concentrations after mixing) and its subsequent reoxidation by 1,4-naphthoquinone were monitored at 0–1.0 s (A), and 0–20 s (B) timescales. Concentrations of 1,4-naphthoquinone after mixing: none (1), 50 μM (2), 100 μM (3), and 150 μM (4).

oxidized state than $HbFe^{2+}O_2$ moiety, *i.e.,* the former acts as a preferential electron donor for the quinone.

3.3. Kinetics of steady-state reduction of quinones and nitroaromatic compounds by SaFHb

We examined the *Sa*FHb-catalyzed reduction of two series of electron acceptors, quinones and nitroaromatic compounds, whose single-electron reduction potentials (E_7^1) vary from 0.08 V to − 0.49 V. We determined the reduction rate constants, $k_{cat(app)}$, at 50 μM NADH, and k_{cat}/K_m (Table 1).

The use of one of the most efficient electron acceptors, juglone (5-hydroxy-1,4-naphthoquinone) (Table 1) revealed that at varied concentrations of juglone and fixed concentrations of NADH, a series of the parallel lines was obtained in double-reciprocal plots (Fig. 5). This indicates that the quinone reductase reaction of FHb follows a'ping-pong' mechanism. The k_{cat} value for juglone reduction, obtained by extrapolation to infinite NADH concentration, is equal to 50.0 ± 7.0 s^{-1}, and the k_{cat}/K_m for NADH is equal to 5.3 ± 0.5 × 10^5 M^{-1} s^{-1}. This value is close to k_{cat}/K_m for NADH obtained in the presteady-state experiments (Fig. 2; 5.6 ± 0.4 × 10^5 $M^{-1}s^{-1}$). At fixed juglone concentration, the reaction product NAD^+ acted as a competitive inhibitor towa rds NADH (Fig. 6A) with K_{is} = 750 ± 120 μM as deduced from Eq. (2). In turn, at fixed concentration of NADH, 50 μM, NAD^+ acted as an uncompetitive inhibitor towards juglone with K_{ii} = 1250 ± 150 μM as deduced from Eq. (3) (Fig. 6B). These data show that NAD^+ binds to the oxidized FHb presumably at the NAD(H)-binding site, and does not efficiently bind to the enzyme reduced state.

We found that the reactivity (k_{cat}/K_m) of aromatic nitrocompounds increases with an increase in their E_7^1 (Table 1, Fig. 7). Although the reactivity of the majority of quinones also shows a trend to increase upon an increase in their E_7^1, derivatives of 2-hydroxy-1,4-naphthoquinone are far more reactive that their counterparts with the similar values of E_7^1 (Fig. 7).

3.4. Single- and two-electron reduction of quinones and nitroaromatic compounds by SaFHb

It is also important to characterize the nature of the electron flux during the reduction of quinones and nitroaromatics by *Sa*FHb. For quinone reduction by NAD(P)H-oxidizing flavoenzymes, the single-electron flux is defined as a ratio of the rate of 1,4-benzoquinone-

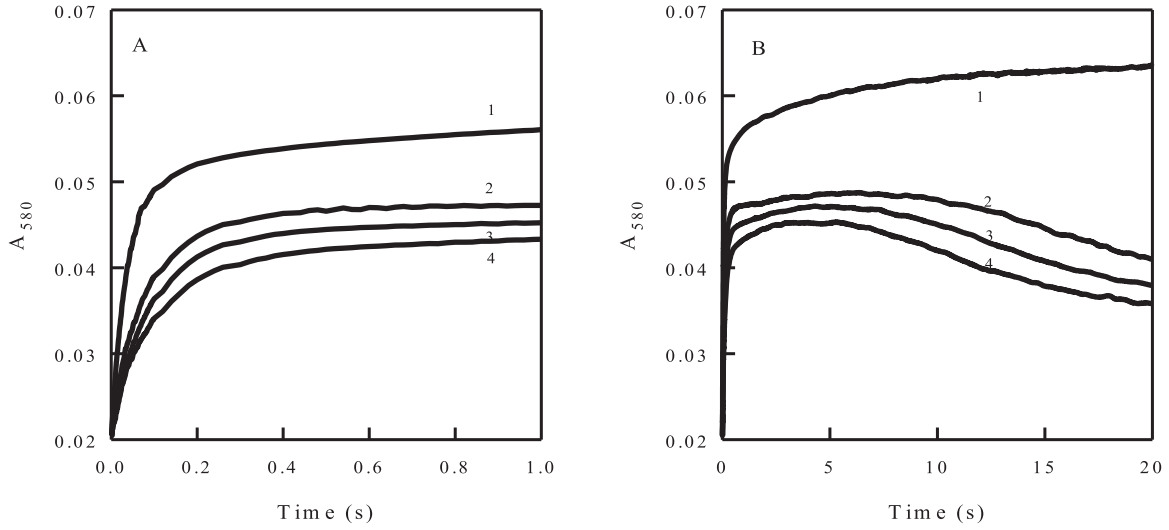

Fig. 4. Turnover of SaFHb in the presence of NADH and 1,4-naphthoquinone under aerobic conditions monitored at 580 nm. The reduction of the *Sa*Fhb $HbFe^{3+}$ (5.0 μM) by 100 μM NADH (concentrations after mixing) and the subsequent reoxidation of $HbFe^{2+}O_2$ by 1,4-naphthoquinone were monitored at 0–1.0 s (A), and 0–20 s (B) timescales. Concentrations of 1,4-naphthoquinone after mixing: none (1), 50 μM (2), 100 μM (3), and 150 μM (4).

Table 1
Steady-state rate constants of quinone and nitroaromatic compounds reduction by *Sa*FHb. [NADH] = 50 μM, 0.1 M K-phosphate + 1.0 mM EDTA, pH 7.0, 25 °C.

No. Compound	E_7^1 (V) [35]	$k_{cat(app)}$ (s^{-1})	k_{cat}/K_m (M^{-1} s^{-1})
a) Quinones			
1. 1,4-Benzoquinone	0.08	25.5 ± 3.0	7.7 ± 0.2 x 10^5
2. 2-Methyl − 1,4-benzoquinone	0.01	21.5 ± 2.5	1.1 ± 0.2 x 10^6
3. 2,6-Dimethyl − 1,4-benzoquinone	− 0.08	10.6 ± 1.2	3.2 ± 0.3 x 10^5
4. 5-Hydroxy − 1,4-naphthoquinone	− 0.09	19.0 ± 2.0	6.1 ± 0.8 x 10^6
5. 5,8-Dihydroxy − 1,4-naphthoquinone	− 0.11	9.3 ± 0.4	2.7 ± 0.3 x 10^5
6. 9,10-Phenanthrene quinone	− 0.12	7.7 ± 0.5	2.7 ± 0.3 x 10^6
7. 1,4-Naphthoquinone	− 0.15	18.1 ± 1.2	2.8 ± 0.5 x 10^5
8. 2-Methyl − 1,4-naphthoquinone	− 0.20	23.0 ± 1.5	1.6 ± 0.2 x 10^5
9. 9,10-Anthraquinone − 2,6-disulfonate	− 0.25	1.2 ± 0.3	1.2 ± 0.2 x 10^4
10. Tetramethyl − 1,4-benzoquinone	− 0.26	4.6 ± 0.3	4.5 ± 0.3 x 10^4
11. 1-Hydroxy − 9,10-anthraquinone	− 0.39	0.3 ± 0.05	3.7 ± 0.3 x 10^4
12. 2-Hydroxy − 1,4-naphthoquinone	− 0.41	12.0 ± 0.7	1.7 ± 0.3 x 10^6
13. 2-Hydroxy − 3-methyl − 1,4-naphthoquinone	− 0.46	1.7 ± 0.2	1.7 ± 0.2 x 10^5
b) Aromatic nitrocompounds			
14. 2,4,6-Trinitrotoluene	− 0.25	18.0 ± 2.0	1.1 ± 0.25 x 10^5
15. 1,4-Dinitrobenzene	− 0.26	25.4 ± 2.0	7.0 ± 0.8 x 10^4
16. 1,2-Dinitrobenzene	− 0.29	7.9 ± 1.5	5.8 ± 0.2 x 10^4
17. 4-Nitrobenzaldehyde	− 0.33	11.8 ± 1.5	1.9 ± 0.3 x 10^4
18. 1,3-Dinitrobenzene	− 0.35	17.9 ± 3.0	8.7 ± 1.2 x 10^4
19. 4-Nitroacetophenone	− 0.36	7.5 ± 1.0	2.2 ± 0.1 x 10^4
20. 4-Nitrobenzyl alcohol	− 0.42	2.6 ± 0.3	2.4 ± 0.4 x 10^3
21. Nitrobenzene	− 0.49	4.7 ± 0.6	6.2 ± 0.6 x 10^2

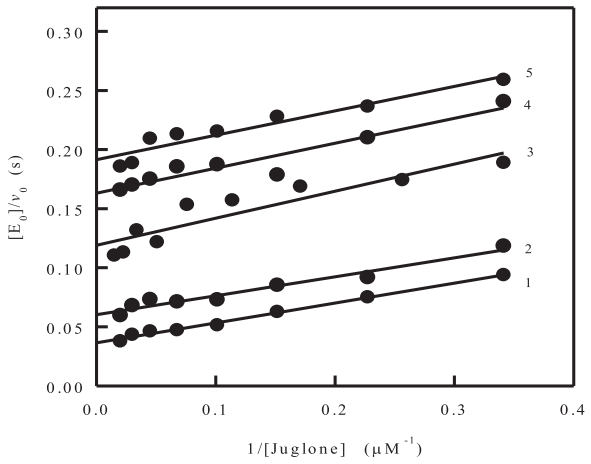

Fig. 5. The 'ping-pong' mechanism of juglone reduction by *S. aureus* FHb. The rates of the *Sa*FHb-catalyzed oxidation of NADH were measured with increasing concentration of juglone. Concentrations of NADH: 100 μM (1), 65 μM (2), 25 μM (3), 19 μM (4), and 13 μM (5).

mediated reduction of the added cytochrome *c* with the doubled rate of 1,4-benzoquinone-mediated NAD(P)H enzymatic oxidation at pH < 7.2 ([36], and references therein). This approach is based on the fast reduction of cytochrome *c* by 1,4-benzosemiquinone ($k \sim 10^6$ M^{-1} s^{-1}), and its slow reduction by the hydroquinone form [36]. The rates presented below were obtained after the substraction of the intrinsic rates of cytochrome *c* reduction by *Sa*FHb in the absence of the electron acceptor. We found that for 1,4-benzoquinone reduction, the single-electron flux was equal to 34 ± 4.0% of the total flux. The assessment of the single-electron flux in the reduction of aromatic nitrocompounds is more complex, because cytochrome *c* may be reduced by both $ArNO_2^{\cdot-}$ (undergoing the rapid redox equilibrium with $O_2/O_2^{\cdot-}$), and by the products of two(four) electron reduction of $ArNO_2$, hydroxylamines [37]. We found that, in the presence of 50 μM NADH and 300 μM TNT or *p*-nitrobenzaldehyde, the rate of *Sa*FHb-catalyzed reduction of added 50 μM cytochrome *c* was equal to 35.3 ± 2.0% and 40.3 ± 2.5% of the doubled NADH oxidation rate, respectively. These reactions were inhibited by 100 U/ml superoxide dismutase by 18% and 86%, respectively. Thus, if expressed as the $O_2^{\cdot-}$-mediated reduction of cytochrome *c,* the single-electron flux comprises 6.3% in the reduction of TNT, and 34.6% in the reduction of *p*-nitrobenzaldehyde. We suggest that the percentage of the single-electron flux is closer to the latter value, 34.6%, because in redox equilibrium with $O_2/O_2^{\cdot-}$, $TNT^{\cdot-}$ (E_7^1 = −0.25 V) will yield a lower amount of $O_2^{\cdot-}$ as compared with the anion-radical of *p*-nitrobenzaldehyde (E_7^1 = −0.33 V). Thus, the TNT-mediated reduction of cytochrome *c* should be less sensitive to the action of SOD [38]. Taken together, our results show that *Sa*FHb performs a mixed single- and two-electron reduction of quinones and nitroaromatic compounds.

3.5. Influence of the FHb azole inhibitors on the kinetics of quinone reduction

We studied the influence of FHb inhibitors miconazole, econazole, and ketoconazole on the kinetics of quinone reduction. Interestingly, these compounds activated this reaction (Fig. 8A). At fixed quinone concentration, they increased the k_{cat}/K_m value for NADH by decreasing the K_m value without increasing the k_{cat} value (Fig. 8A). The presentation of the activation efficiency *vs.* the activator concentration in double-reciprocal plots (Fig. 8B) showed that the maximal activation degree ($1/\alpha$, Eq.(4)) with respect to the k_{cat}/K_m value of NADH in all three cases was close to 20, and that the K_a values of azole compounds were 4.4 ± 0.5 μM (miconazole), 33.0 ± 5.0 μM (econazole), and 71.0 ± 9.0 μM (ketoconazole).

At 50 μM NADH, these compounds did not alter the k_{cat}/K_m value for juglone reduction, although they increased the maximal reaction rates (data not show), due to a decrease of the K_m for NADH. These results show that the above compounds increase the NADH affinity towards the oxidized enzyme form, but do not affect the reactivity of quinoidal oxidant. Analogosusly, micromolar concentrations of miconazole activated the reduction of another examined oxidant, 2-hydroxy-1,4-naphthoquinone. In contrast, another inhibitor of FHb, cyanide which binds to the heme moiety at micromolar concentrations [39], did not stimulate quinone reduction. At fixed juglone concentration, 50 μM, 1 mM KCN decreased k_{cat}/K_m for NADH by 15 ± 5%, and did not affect the k_{cat} of reaction (data not shown).

4. Discussion

FHb takes part in the neutralization of nitrosative stress in the bacterial cell [7]. Thus, the inhibition or subversion of its functions may be considered as a potential approach for antibacterial chemotherapy. The redox active quinones and nitroaromatic compounds, which may generate ROS during their redox cycling initiated by FHb, may counteract its physiological functions, namely may increase the rate of formation of toxic peroxynitrite. The present study discloses several important features of catalysis of *Sa*FHb, and characterizes the mechanism of its reactions with the above groups of non-physiological oxidants.

First, we extended the characterization of *Sa*FHb kinetics, which, to the best of our knowledge, was limited to studies of NADH: oxidase, ferricyanide or cytochrome *c* reductase, and $NO^{\cdot}$ dioxygenase activities under steady-state conditions [20,33]. Our presteady-state data (Fig. 2) show that the reduction of FAD, the subsequent reduction of $HbFe^{3+}$, and the formation of $HbFe^{2+}O_2$ proceed with almost equal rates, ~130 s^{-1}, *i.e.,* the formation of $HbFe^{2+}$ and the subsequent oxygen binding are much faster than the reduction of FAD. This value also

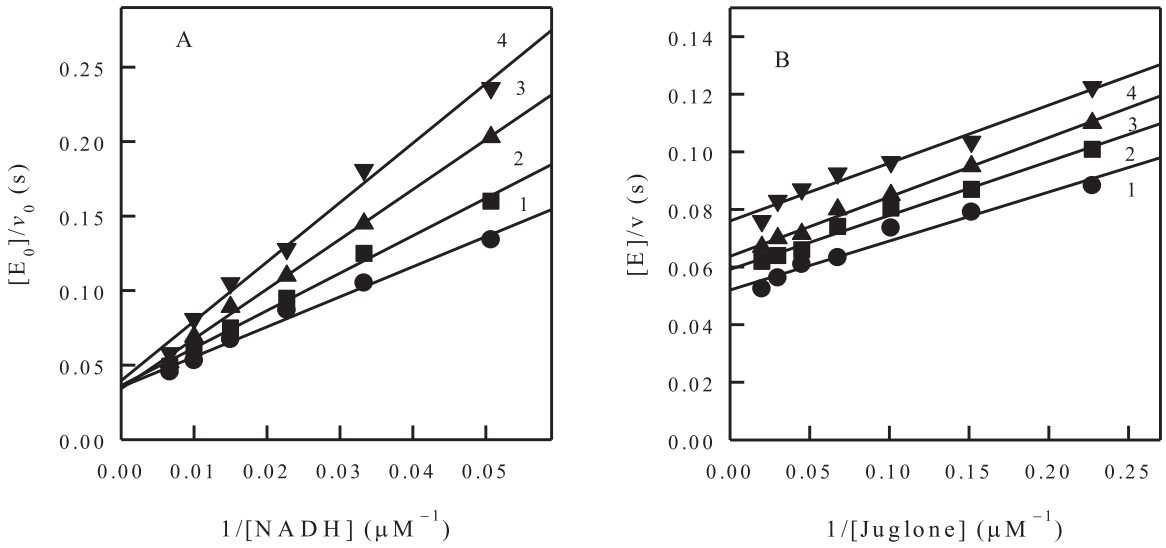

Fig. 6. Inhibition by NAD^+ of the quinone reductase reaction of *S. aureus* FHb. (A) Inhibition at varied NADH concentrations in the presence of 50 μM juglone. NAD^+ concentrations: 0 mM (1), 0.2 mM (2), 0.4 mM (3), and 0.6 mM (4). (B) Inhibition at varied juglone concentrations in the presence of 50 μM NADH. NAD^+ concentrations: 0 mM (1), 0.2 mM (2), 0.4 mM (3), and 0.6 mM (4).

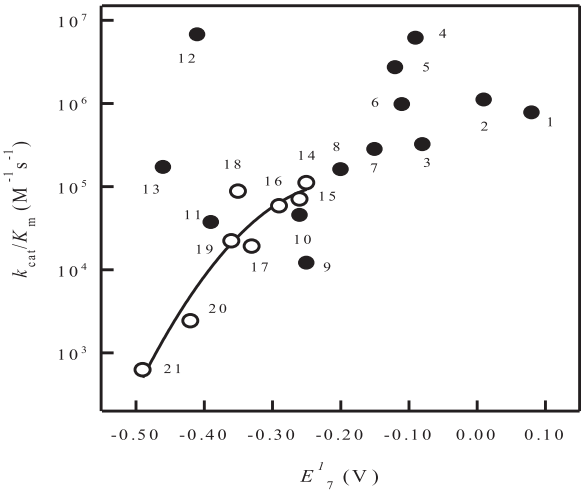

Fig. 7. Dependence of the reactivity of quinones and nitroaromatic compounds on their single-electron reduction potential. Relationship between log k_{cat}/K_m of quinones (solid circles) and nitroaromatic compounds (blank circles) and their single-electron reduction potentials at pH 7.0 (E_7^1). Numbers refer to quinones and nitroaromatic compounds whose redox potentials and reduction rate constants are given in Table 1.

enables us to indirectly assess the rate of $NO^{\cdot}$ dioxygenation step for this enzyme. Since, at pH 7.5, the steady-state NADH-dependent $NO^{\cdot}$ dioxygenation by SaFHb has a maximal rate of 66 s^{-1} [33], then the maximal rate of this step is close to 130 s^{-1}.

For other FHbs, kinetic studies of intramolecular electron-transfer are scarce. Based on presteady-state kinetics, the rate constant of $FADH^{\cdot}$-to- heme electron transfer in *E. coli* FHb was proposed to be about 150 s^{-1} (pH 7.0, 20 °C) [8]. However, it is likely that this process is limited by the previous step, namely FAD reduction by NADH [8], as in our case. Pulse-radiolysis study of *R. eutropha* FHb gave a rate constant of $FADH^{\cdot}$-to-heme intramolecular electron-transfer of 6.8×10^3 s^{-1} at pH 7.0 [34]. Further insight into the mechanism of intramolecular electron transfer in *Sa*FHb is complicated by an uncertainty about its $FADH^{\cdot}$ stability. There are only limited data on FHbs redox potentials for comparison (Table 2).

The amino acid residues surrounding the FAD isoalloxazine ring and their interactions with its heteroatoms are conserved between *S. aureus, R. eutropha,* and *E. coli* FHbs [5,20]. Thus, one may expect that the amount of FADH. stabilized at equilibrium in *Sa*FHb does not significantly differ from that in *E. coli* FHb, namely 15% [40]. In this case, the midpoint potential for $FAD/FADH^-$ (Table 2) after a correction for pH 7.0 is equal to − 0.172 V, and a calculation according to the Nernst equation give the following redox potential values: $E_7(FAD/FADH^{\cdot}) \leq -0.198$ V, and $E_7(FADH^{\cdot}/FADH^-) \geq -0.146$ V. Thus, due to the thermodynamic reasons, the electron transfer from $FADH^{\cdot}$ to heme should be faster than the electron transfer from $FADH^-$ to heme. By comparison with *R. eutropha* FHb [34], one may expect the rate constant of $FADH^-$ -to-heme electron-transfer in *Sa*FHb to be on the order of $\geq 10^3$ s^{-1}.

Next, we characterized the reactivity of SaFHb towards quinones and nitroaromatics. The data of Figs. 3,4 demonstrate that, during the enzyme turnover, quinones preferentially oxidize reduced FAD rather than $HbFe^{2+}O_2$. In general, the ease of oxidation of a particular prosthetic group depends on its redox potential and on its accessibility which affects its intrinsic reactivity, *i.e.,* the electron self-exchange rate constant [41]. The crystal structures of FHb from various sources [5,18,19] show that the pyrimidine ring of the FAD isoalloxazine is partly accessible to solvent, whereas access to the heme may be partly hampered by a bound phospholipid molecule [5,19,33]. Besides, although the redox potentials of FAD and iron couples of *Sa*FHb are sufficiently close [33], the binding of O_2 which is characterized by a submicromolar K_d value [8], may significantly increase the potential of $HbFe^{3+}/HbFe^{2+}O_2$ redox couple and impede $HbFe^{2+}O_2$ oxidation by quinones. The 'ping-pong' mechanism of quinone reduction by *Sa*FHb (Fig. 5) shows that reductive and oxidative half-reactions take place independently. The $k_{cat(app)}$ of reactions at 50 μM NADH (Table 1) in most cases were lower than the FAD reduction rate in presteady-state experiments (Fig. 2). This shows that the oxidative half-reaction is rate-limiting in catalysis, with a possible exception of 1,4-benzoquinone, 2-methyl-1,4-naphthoquinone, and 1,4-dinitrobenzene, where the reductive half-reaction may be partly rate-limiting. The competitive inhibition exerted by the reaction product, NAD^+, with respect to NADH (Fig. 6A), and the uncompetitive inhibition with respect to an oxidant juglone (Fig. 6B) are in line with a 'ping-pong' mechanism, where NAD^+ binds relatively tightly to the oxidized enzyme form, but binds weakly or not at all to reduced *Sa*FHb [42].

Another important feature of *Sa*FHB is the mixed single- and two-electron reduction of quinones and nitroaromatic compounds favoring the two-electron transfer, which is not characteristic for flavoenzymes

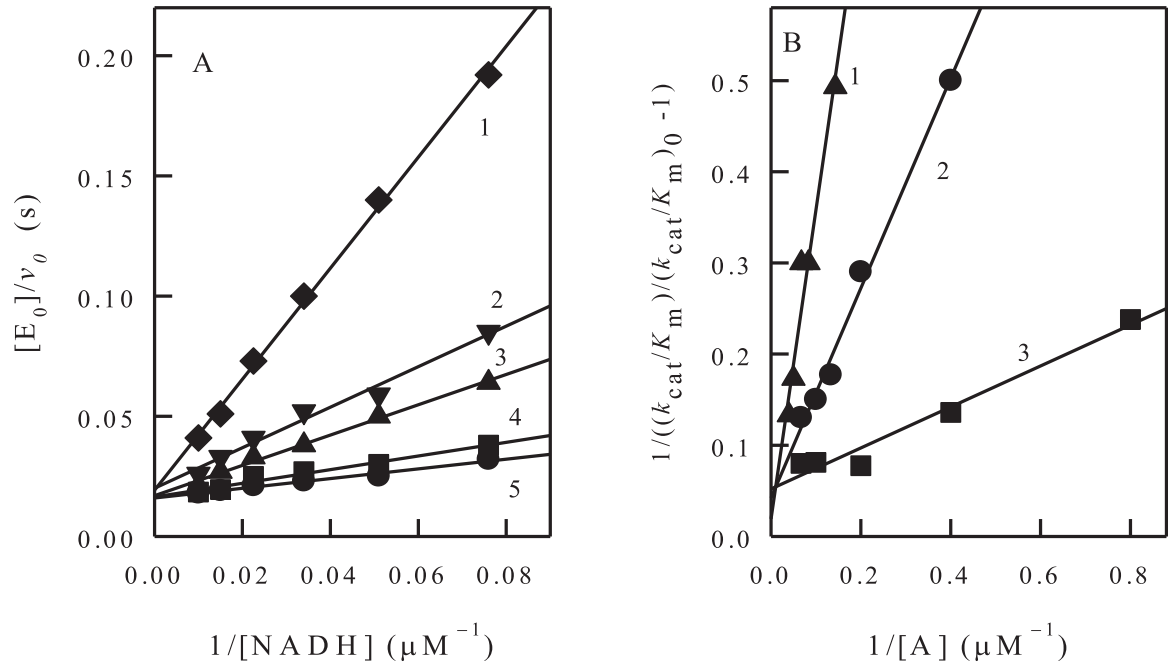

Fig. 8. Activation by azole inhibitors of the quinone reductase reaction of *S. aureus* FHb. (A) Increase in k_{cat}/K_m for NADH in *Sa*FHb-catalyzed reduction of juglone (50 μM) in the presence of ketoconazole. Compound concentrations: none (1), 7.5 μM (2), 15 μM (3), 20 μM (4), and 25 μM (5). (B) Dependence of the reaction activation degree $((k_{cat}/K_m)/(k_{cat}/K_m)_0 - 1)$ on the concentration of ketoconazole (1), econazole (2), and miconazole (3).

Table 2
Midpoint potentials (E°) of flavohemoglobins from various species.

No.	Species	E^0 (V) FAD/FADH$^-$	E^0 (V) $HbFe^{3+}/HbFe^{2+}$	Conditions
1.	*E. coli*	≤ −0.15	− 0.12	pH 8.0 [40]
2.	*S. aureus*	− 0.19	− 0.17	pH 7.6 [33]
3.	*R. eutropha*	n.d.	− 0.15	pH 7.0 [39]

dehydrogenases-electrontransferases [27,28]. One case is that of the *Anabaena* FNR Glu301Ala variant where the reduction of quinones acquires partly two-electron character upon FADH. destabilization [43]. Taking into account the low stability of FADH. in FHbs, for *Sa*FHb we can propose a scheme of mixed single- and two-electron reduction of quinones by FADH$^-$ and FADH. redox states without the involvement of $HbFe^{2+}O_2$ (Scheme 1).

Our data provide some insight on the specificity of *Sa*FHb towards quinoidal and nitroaromatic oxidants. The single-electron reduction of the above oxidants by flavoenzymes dehydrogenases-electrontransferases, *e.g.,* NADPH:cytochrome P-450 reductase, FNR, and NO-synthase follows an 'outer-sphere' electron-transfer mechanism [41]. Their quantitative structure-activity relationships are relatively easy to understand – the log k_{cat}/K_m of the reactions for different oxidants is relatively insensitive to their structure and increases with an increase in their E_7^1. Also the reactivity of quinones is typically higher than that of nitroaromatics that possess similar E_7^1 values ([28], and references therein). This is because the electron self-exchange constants of quinones, ~10^8 M^{-1} s^{-1}, are much higher than those of nitroaromatic compounds, ~10^6 M^{-1} s^{-1} [22]. The data of Fig. 7 show that the reactivity of *Sa*FHb partly follows these rules, *i.e.,* the log k_{cat}/K_m of nitroaromatics displays a well expressed parabolic dependence on their E_7^1, and is systematically lower than log k_{cat}/K_m of quinones. However, the dependence of log k_{cat}/K_m of quinones on their E_7^1 is not well defined, with a significantly enhanced reactivity of 2-hydroxy-1,4-naphthoquinones. The nature of this phenomenon is currently unclear and deserves further studies. It most likely depends on the structural

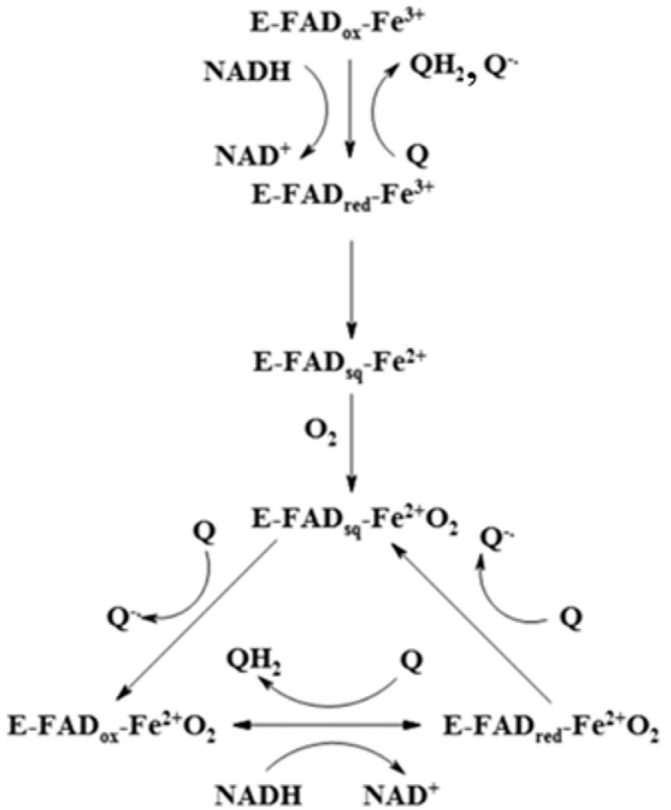

Scheme 1. Mixed single- and two-electron reduction of quinones by FADH$^-$ and FADH.redox states occurring at short times.

pecularities of the FAD surroundings of *Sa*FHb. For example, it is also characteristic for reactions of *E. coli* nitroreductase A [42].

Finally, the possible biomedical implications of the reduction of quinones and nitroaromatics by *Sa*FHb deserve discussion. In terms of k_{cat}/K_m of quinone reduction, the reactivity of *Sa*FHb (Table 1, Fig. 7) is

relatively high as compared with other flavodehydrogenases-electrontransferases, with the following order: NADPH:cytochrome P-450 reductase [27] > *Sa*FHb > FNR [27] ≥ neuronal NO-synthase [28] > mitochondrial complex I [26]. An important property of SaFHb is enhanced reduction of low-potential 2-hydroxy-1,4-naphthoquinones (Fig. 7); these compounds are poor substrates for mammalian flavodehydrogenases-electrontransferases [26,28], and possess low toxicity in mammalian cells [21]. Thus, irrespective of a significant percentage of two-electron flux in the reduction of oxidant, *Sa*FHb is a potentially efficient source of free radicals of quinoidal and nitroaromatic compounds with possible chemotherapeutic importance. Indeed, quinones would impede the $NO^{\cdot}$ dioxygenation by *Sa*FHb by intercepting the electron flux from the reduced FAD thus slowing down the reduction of $HbFe^{3+}$ (Fig. 4B). The stimulation of quinone reduction of *Sa*FHb, exerted by its azole inhibitors, is a particularly important result (Fig. 8A,B). These compounds are ligated to the heme iron *via* the imidazole *N*1 atom [17,18]. Concomitantly, their binding induces the rotation of the NADH binding domain up to 30°, which implies a narrower cleft between the FAD and NADH domains [17]. This may possibly ensure a tighter binding of NADH to FAD, which is reflected by a decrease of the NADH K_m value (Fig. 8A). Taken together, these findings imply that the combined use of the azole inhibitors of FHb and of quinones may be a highly promising approach in antimicrobial chemotherapy.

In conclusion, our study for the first time identified *S. aureus* flavohemoglobin as a potent quinone- and nitroreductase. This enzyme reduces these compounds in a mixed single- and two-electron process. *Sa*FHb is characterized by an unusual oxidizing substrate specificity for low-potential 2-hydroxy-1,4-naphthoquinones. The rates of these reactions in most cases are limited by the oxidative half-reaction. Based on the steady- and presteady-state experiments, a scheme of the enzyme turnover has been proposed involving the preferential oxidation of the reduced FAD rather than of Hb-$Fe^{2+}O_2$ cofactor by quinones. Taken together with the activation of quinone reduction by the azole inhibitors of *Sa*FHb, these data suggest the potential usefulness of the combined use of quinones and FHb inhibitors in antibacterial chemotherapy.

Acknowledgments

This study was in part supported by the collaborative Gilibert grant between the French Ministère des Affaires Etrangères (28443UK) and the Scientific Council of Lithuania (No. TAP LZ 07/2013).

References

[1] A. Bonamore, A. Boffi, Flavohemoglobin: structure and reactivity, IUBMB Life 60 (2008) 19–28.
[2] A.D. Frey, P.T. Kallio, Bacterial hemoglobins and flavohemoglobins: versatile proteins and their impact on microbiology and biotechnology, FEMS Microbiol. Rev. 27 (2003) 525–545.
[3] M.T. Forrester, M.W. Foster, Protection from nitrosative stress: a central role for microbial flavohemoglobin, Free Rad. Biol. Med. 52 (2012) 1620–1633.
[4] P.R. Gardner, Hemoglobin: a nitric-oxide dioxygenase, Scientifica (2012) 1–34.
[5] U. Ermler, R.A. Siddiqui, R. Cramm, B. Friedrich, Crystal structure of the flavohemoglobin from *Alcaligenes eutrophus* at 1.75 Å resolution, EMBO J. 14 (1995) 6067–6077.
[6] S.G. Andrews, D. Shipley, J.N. Keen, J.B.C. Findlay, P.M. Harrison, J.R. Guest, The haemoglobin-like protein (HMP) of *Escherichia coli* has a ferrisiderophore reductase activity and its *C*-terminal domain shares homology with ferredoxin:nadp$^+$ reductase, FEBS Lett. 302 (1992) 247–252.
[7] P.R. Gardner, A.M. Gardner, L.A. Martin, A.L. Salzman, Nitric oxide dioxygenase: an enzymic function for flavohemoglobin, Proc. Natl. Acad. Sci. USA 95 (1998) 10378–10383.
[8] A.M. Gardner, L.A. Martin, P.R. Gardner, Y. Dou, J.S. Olson, Steady-state and transient kinetics of *Escherichia coli* nitric-oxide dioxygenase (flavohemoglobin). The B10 tyrosine hydroxyl is essential for dioxygen binding and catalysis, J. Biol. Chem. 275 (2000) 12581–12589.
[9] A.M. Firoved, S.R. Wood, W. Omatowski, V. Deretic, G.S. Timmins, Microarray analysis and functional characterization of the nitrosative stress response in nonmucoid and mucoid *Pseudomonas aeruginosa*, J. Bacteriol. 186 (2004) 4046–4050.
[10] C. Gras-Le Guen, A. Jarry, G. Vallette, C. Toquet, C. Colombeix, C.L. Laboisse, G. Potel, J.C. Roze, D. Bugnon, T. Debillon, Antibiotic therapy reduces nitrosative stress and programmed cell death in the rabbit foetal lung, Eur. Respir. J. 25 (2005) 88–95.
[11] S.K. Fridkin, J.C. Hageman, M. Morrison, L.T. Sanza, K. Como-Sabetti, J.A. Jernigan, K. Harriman, L.H. Harrison, R. Lynfield, M.M. Farley, Methicillin-resistant *Staphylococcus aureus* disease in three communities, N. Engl. J. Med. 352 (2005) 1436–1444.
[12] A.R. Richardson, P.M. Dunman, F.C. Fang, The nitrosative stress response of *Staphylococcus aureus* is required for resistance to innate immunity, Mol. Microbiol. 61 (2006) 927–939.
[13] A.R. Richardson, S.J. Libby, F.C. Fang, A nitric oxide-inducible lactate dehydrogenase enables *Staphylococcus aureus* to resist innate immunity, Science 319 (2008) 1672–1676.
[14] L.S. Nobre, S. Todorovic, A.F.N. Tavares, E. Oldfield, P. Hildebrandt, M. Teixeira, L.M. Saraiva, Binding of azole antibiotics to *Staphylococcus aureus* flavohemoglobin increases intracellular oxidative stress, J. Bacteriol. 192 (2010) 1527–1533.
[15] K.J. McLean, K.R. Marshall, A. Richmond, I.S. Hunter, K. Fowler, T. Kieser, S.S. Gurcha, G.S. Besra, A.W. Munro, Azole antifungals are potent inhibitors of cytochrome P450 mono-oxygenase and bacterial growth in mycobacteria and streptomycetes, Microbiology 148 (2002) 2937–2949.
[16] R. Becher, S.G. Wiesel, Fungal cytochrome P450 sterol 14a-demethylase (CYP51) and azole resistance in plant and human pathogens, Appl. Microbiol. Biotechnol. 95 (2012) 825–840.
[17] R.A. Helmick, A.E. Fletcher, A.E. Gardner, C.R. Gessner, A.N. Hvitved, M.C. Gustin, P.R. Gartner, Imidazole antibiotics inhibit the nitric oxide dioxygenase function of microbial flavohemoglobin, Antimicrob. Agents Chemother. 49 (2005) 1837–1843.
[18] E. El Hammi, E. Warkentin, U. Demmer, F. Limam, N.M. Marzouki, U. Ermler, L. Baciou, Structure of *Ralstonia eutropha* flavohemoglobin in complex with three antibiotic azole compounds, Biochemistry 50 (2011) 1255–1264.
[19] E. El Hammi, E. Warkentin, U. Demmer, N.M. Marzouki, U. Ermler, L. Baciou, Active site analysis of yeast flavohemoglobin based on its structure with a small ligand or econazole, FEBS J. 279 (2012) 4565–4575.
[20] A. Ezzine, M. Moussaoui, E. El Hammi, M.N. Marzouki, L. Baciou, Antimicrobial agents act differently on *Staphyloccocus aureus* and *Ralstonia eutropha* flavohemoglobins, Appl. Biochem. Biotechnol. 173 (2014) 1023–1037.
[21] P.J. O'Brien, Molecular mechanisms of quinone cytotoxicity, Chem. -Biol. Interact. 80 (1991) 1–41.
[22] P. Wardman, I. Wilson, Control of the generation of free radicals in biological systems by kinetic and thermodynamic factors, Free Radic. Res. Commun. 2 (1987) 225–232.
[23] P. Wardman, M.F. Dennis, S.A. Everet, K.B. Patel, M.R.L. Stratford, M. Tracy, Radicals from one-electron reduction of nitro compounds, aromatic *N*-oxides and quinones: the kinetic basis for hypoxia-selective, bioreductive drugs, Biochem. Soc. Symp. 61 (1995) 171–194.
[24] J. Koyama, Anti-infective quinone derivatives of recent patents, Recent Pat. Antiinfect. Drug Discov. 1 (2006) 113–125.
[25] P. Kovacic, R. Somanathan, Nitroaromatic compounds: environmental toxicity, carcinogenicity, mutagenicity, therapy and mechanism, J. Appl. Toxicol. 34 (2014) 810–824.
[26] D.A. Bironaitė, N.K. Čėnas, J.J. Kulys, The rotenone-insensitive reduction of quinones and nitroaromatic compounds by mitochondrial NADH: quinone reductase, Biochim. Biophys. Acta 1060 (1991) 203–209.
[27] N. Čėnas, Ž. Anusevičius, H. Nivinskas, L. Misevičienė, J. Šarlauskas, Structure-activity relationships in two-electron reduction of quinones, Meth. Enzymol. 382 (B) (2004) 258–277.
[28] Ž. Anusevičius, H. Nivinskas, J. Šarlauskas, M.-A. Sari, J.-L. Boucher, N. Čėnas, Single-electron reduction of quinone and nitroaromatic xenobiotics by recombinant rat neuronal nitric oxide synthase, Acta Biochim. Pol. 60 (2013) 217–222.
[29] J. Marcinkevičienė, N. Čėnas, J. Kulys, S.A. Usanov, N.M. Sukhova, I.S. Selezneva, V.F. Gryazev, Nitroreductase reactions of the NADPH:adrenodoxin reductase and the adrenodoxin complex, Biomed. Biochim. Acta 49 (1990) 167–172.
[30] P.R. Smith, R.I. Krohn, G.T. Hermanson, A.K. Mallia, F.H. Gartner, M.D. Provenzano, E.K. Fujimoto, N.M. Goeke, B.J. Olson, D.C. Klenk, Measurement of protein using bicinchoninic acid, Anal. Biochem. 150 (1985) 76–85.
[31] V. Leskovac, Comprehensive Enzyme Kinetics, Kluwer Academic Publishers, New York, Boston, Dordrecht, London, Moscow, 2003.
[32] P.V. Patil, D. Ballou, The use of protocatechuate dioxygenase for maintaining anaerobic conditions in biochemical experiments, Anal. Biochem. 286 (2000) 187–192.
[33] L.S. Nobre, V.L. Goncalves, L.M. Saraiva, Flavohemoglobin of *Staphylococcus aureus*, Methods Enzymol 436 (2008) 203–216.
[34] E. El Hammi, C. Houee-Levin, J. Rezač, B. Levy, I. Demachy, L. Baciou, A. de la Lande, New insights into the mechanism of electron transfer within flavohemoglobins: tunnelling pathways, packing density, thermodynamic and kinetic analyses, Phys. Chem. Chem. Phys. 14 (2012) 13872–13880.
[35] P. Wardman, Reduction potentials of one-electron couples involving free radicals in aqueous solutions, J. Phys. Chem. Ref. Data 18 (1989) 1637–1755.
[36] T. Iyanagi, On the mechanism of one-electron reduction of quinones by microsomal flavin enzymes: the kinetic analysis between cytochrome b5 and menadione, Free Radic. Res. Commun. 8 (1990) 259–268.
[37] J. Šarlauskas, A. Nemeikaitė-Čėnienė, Ž. Anusevičius, L. Misevičienė, M. Julvez, M. Medina, C. Gomez-Moreno, N. Čėnas, Flavoenzyme-catalyzed redox cycling of hydroxylamino- and amino metabolites of 2,4,6-trinitrotoluene: implications for their cytotoxicity, Arch. Biochem. Biophys. 425 (2004) 184–192.
[38] J. Butler, B.M. Hoey, The apparent inhibition of superoxide dismutase activity by

quinones, J. Free Radic. Biol. Med. 2 (1986) 77–81.
[39] P. de Oliveira, A. Ranjbari, L. Baciou, T. Bizouam, G. Ollesch, U. Ermler, P. Sebban, A. Keita, L. Nadjo, Preliminary electrochemical studies of the flavohaemoprotein from *Ralstonia eutropha* entrapped in a film of methyl cellulose: activation of the reduction of dioxygen, Bioelectrochemistry 70 (2007) 185–191.
[40] C.E. Cooper, N. Ioannidis, R. D'mello, R.K. Poole, Haem, flavin and oxygen interactions in Hmp, a flavohaemoglobin from *Escherichia coli*, Biochem. Soc. Trans. 22 (1994) 709–713.
[41] R. Marcus, N. Sutin, Electron transfers in chemistry and biology, Biochim. Biophys. Acta 811 (1985) 265–322.
[42] B. Valiauga, E.M. Williams, D.F. Ackerley, N. Čėnas, Reduction of quinones and nitroaromatic compounds by *Escherichia coli* nitroreductase A (NfsA): characterization of kinetics and substrate specificity, Arch. Biochem. Biophys. 614 (2017) 14–22.
[43] Ž. Anusevičius, L. Misevičienė, M. Medina, M. Martinez-Julvez, C. Gomez-Moreno, N. Čėnas, FAD semiquinone stability regulates single- and two-electron reduction of quinones by *Anabaena* PCC7119 ferredoxin: $NADP^+$ reductase, Arch. Biochem. Biophys. 437 (2005) 144–150.